(e, 2e) electron momentum spectrometer with high sensitivity and high resolution

X. G. Ren, C. G. Ning, J. K. Deng,[a)] S. F. Zhang, G. L. Su, F. Huang, and G. Q. Li
Department of Physics, Tsinghua University, Beijing 100084, People's Republic of China,
Key Laboratory of Atomic and Molecular NanoSciences, Ministry of Education

A high sensitivity and high resolution (e, 2e) electron momentum spectrometer with simultaneous detection in energy and momentum are constructed. The design and performance of the spectrometer are reported. The orbital electron density distributions are obtained accurately and rapidly by using this spectrometer equipped with a double toroidal analyzer. The experimental results on argon and helium exhibit the significant improvements in coincidence count rates, resolution, sensitivity and obtainment of a wide range of adjustable experimental impact energies, which are crucial for further electron momentum spectroscopy studying electronic structure and electron correlation in complex systems. © *2005 American Institute of Physics.*
[DOI: 10.1063/1.1897668]

I. INTRODUCTION

In atoms, molecules and solids the cloud of electrons determines the relative positions of the nuclei. Usually the electron clouds are imaged as a distribution in coordinate space. Since a position space wave function is uniquely related to the corresponding momentum space one by Fourier transformation, the electron clouds can also be equally well imaged as a distribution in momentum space. The picture of the electron clouds as a distribution in momentum space can be directly measured by electron momentum spectroscopy (EMS).[1–4] EMS, also known as binary (e, 2e) spectroscopy, has been developed into a powerful tool for the investigation of orbital electron density distributions and the evaluation and design of electronic wave functions in atoms and molecules. The results of this technique provide the most direct experimental measurements of orbitals and bonding,[4] thus opening fresh and comprehensive studies of electronic structure and electron correlation effects and pole strengths. Furthermore, it is worth noting from a chemical standpoint that EMS provides very direct information on the binding energies, the behavior (motion) of electrons and the electron density in the chemically reactive individual outer valence orbitals and molecular recognition.[5]

However, most EMS studies have been limited to relatively small and stable molecules. While large molecules and chemical interesting low density targets such as free radicals, ions and van der Waals molecules are effectively beyond the reach of existing conventional instruments due to the limitations in sensitivity and resolution, caused by the fact that EMS is a coincidence counting experiment and also that a very large proportion of the available signal is squandered due to limitations in the angular and energy ranges. As a result of these limitations, many new types of experiments are unfeasible within a practical length of time with the existing spectrometers, and their achievement will require major improvement in the sensitivity of EMS. Over the last three decades some of the considerable research efforts in the EMS have been made. One energy dispersive multichannel electron momentum spectrometer has been introduced by McCarthy and Weigold[1,3] with the one-dimensional position sensitive detectors (PSDs). Todd and co-workers have developed a momentum dispersive[6] as well as energy dispersive spectrometers.[7,8] Another important development of multichannel spectrometer has been reported by Moore, Coplan and Skillman,[9] which used a toroidal energy analyzer with an array of channel electron multipliers, allowing simultaneous measurements at a series of azimuthal angles. Recently, multichannel spectrometers with spherical analyzer and two-dimensional PSDs have been reported by Zheng *et al.*[10] with two pairs of resistive anode detectors and Takahashi *et al.*[11]
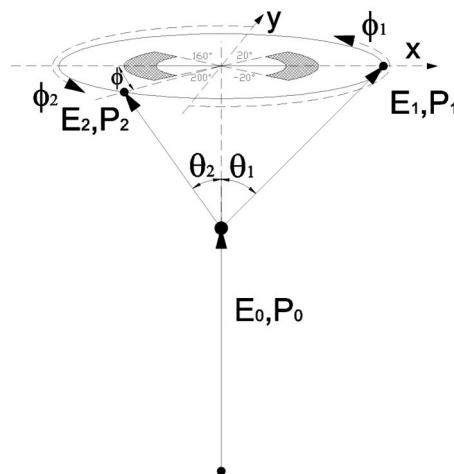
FIG. 1. The (e, 2e) reaction schematic in the symmetric noncoplanar geometry.

[a)]Author to whom correspondence should be addressed; electronic mail: djk-dmp@tsinghua.edu.cn
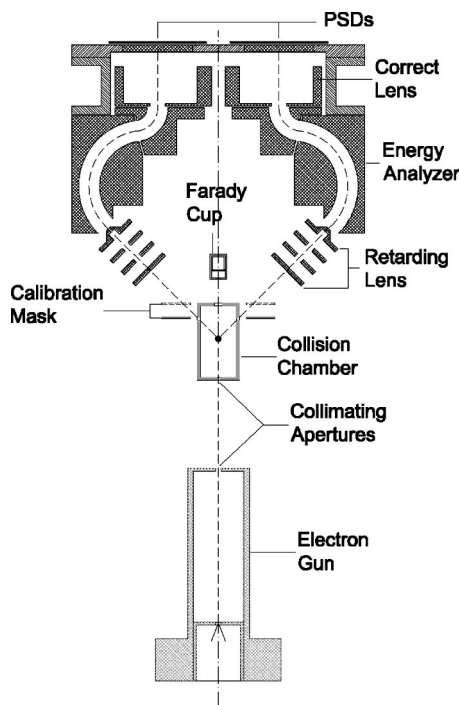
FIG. 2. Cross section schematic of the high sensitivity and high resolution (e, 2e) electron momentum spectrometer.

with a pair of delay-line detectors, respectively. Moreover, high energy electron momentum spectrometers have been developed by Storer and co-workers.[12,13]

In this article the design and performance of the high sensitivity and high resolution electron momentum spectrometer with simultaneous detection in energy and momentum are reported. A double toroidal analyzer (DTA) and a pair of wedge strip anode (WSA) PSDs with a universal serial bus (USB) multi-parameter data-acquisition system[14] are used in the EMS spectrometer. Moreover, a conical retarding lens system is equipped to achieve higher energy resolution. Taking advantage of the DTA analyzer the large fractions of the energy and azimuthal angle range are obtained. The experimental results on argon and helium demonstrated that the coincidence count rates, sensitivity and resolutions were greatly improved.

II. THEORETICAL BACKGROUND

EMS is an (e, 2e) electron impact ionization experiment. A high energy incident electron knocks out an electron from the target atoms or molecules and the two outgoing electrons are subsequently detected in coincidence. The (e, 2e) reaction can be described as

$$e_0 + M \rightarrow M^+ + e_1 + e_2. \tag{1}$$
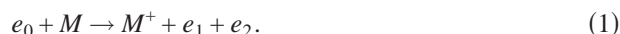
Measuring the incident $E_0, \mathbf{p}_0$ and two outgoing $E_1, \mathbf{p}_1$ and $E_2, \mathbf{p}_2$, electron energies and momenta, respectively, allows the target electron binding energy ε, and target recoil momentum $\mathbf{q}$, to be determined using conservation of energy and momentum

$$\varepsilon = E_0 - E_1 - E_2, \tag{2}$$

$$\mathbf{q} = \mathbf{p}_0 - \mathbf{p}_1 - \mathbf{p}_2. \tag{3}$$

One kinematic geometry which has been mostly used for EMS is noncoplanar symmetric kinematics as shown in Fig. 1. In this kinematics two outgoing electrons have equal scattering polar angles $(\theta_1 = \theta_2 = 45°)$ and equal energies $(E_1 \approx E_2)$. Under high impact energy and high momentum transfer conditions, the plane wave impulse approximation (PWIA) provides a good description of the collision[1–3] and the ionized electron essentially undergoes a clean "knock-out" collision, as prescribed by the binary encounter approximation. In the PWIA the momentum $\mathbf{p}$ of the ejected electron prior to knock-out is equal in magnitude but opposite in sign to the momentum $\mathbf{q}$ of the recoiling ion, i.e., $\mathbf{p} = -\mathbf{q}$. The magnitude of the electron momentum $\mathbf{p}$ is related to ϕ by Eq. (3):

$$p = \left\{ (2p_1 \cos\theta - p_0)^2 + \left[2p_1 \sin\theta \sin\left(\frac{\phi}{2}\right) \right]^2 \right\}^{1/2}, \tag{4}$$

where p_1 and p_0 are the momenta of the outgoing and incident electrons, respectively, and ϕ is the azimuthal angle difference between the two outgoing electrons. To obtain a uniform energy response function, the incident electron energy is usually scanned over a preset region. From the binding energy spectra at different ϕ angles, orbital electron momentum (density) distributions can be obtained.

Under the PWIA the EMS cross section for randomly oriented molecules can be given by

$$\sigma_{\text{EMS}} \propto \int d\Omega |\langle p \Psi_f^{N-1} | \Psi_i^N \rangle|^2, \tag{5}$$

where p is the momentum of the target electron prior to electron ejection. $|\Psi_f^{N-1}\rangle$ and $|\Psi_i^N\rangle$ are the total electronic wave functions for the final ion state and the target molecule ground (initial) state, respectively. The integral represents the spherical average due to the randomly oriented gas phase target in the collision region.[1] The overlap of the ion and neutral wave functions in Eq. (5) is known as the Dyson orbital while the square of this quantity is referred to as an ion-neutral overlap distribution. Thus, the (e, 2e) cross section is essentially proportional to the spherical average of the square of the Dyson orbital in momentum space.[1–3]

By using the target Hartree–Fock approximation (THFA)[3] or the target Kohn–Sham approximation (TKSA),[15] the Dyson orbital can be approximated with the neutral state canonical Hartree–Fock (HF) or Kohn–Sham (KS) orbital. The EMS cross section can be further simplified by

$$\sigma_{\text{EMS}} \propto \int d\Omega |\psi_j(p)|^2, \tag{6}$$

where $|\psi_j(p)\rangle$ is the momentum space canonical HF or KS orbital wave function for the j_{th} electron which was ionized. The integral in Eq. (6) is known as the spherically averaged momentum distribution. Therefore EMS has the ability to image the electron density distribution in individual orbital selected according to their binding energies.

TKSA includes an accounting for initial state electron correlation effects via the density functional theory (DFT) exchange correlation potential. It can be noted that the THFA and TKSA treatments constitute two different levels of the orbital approximation and thus they provide a direct means
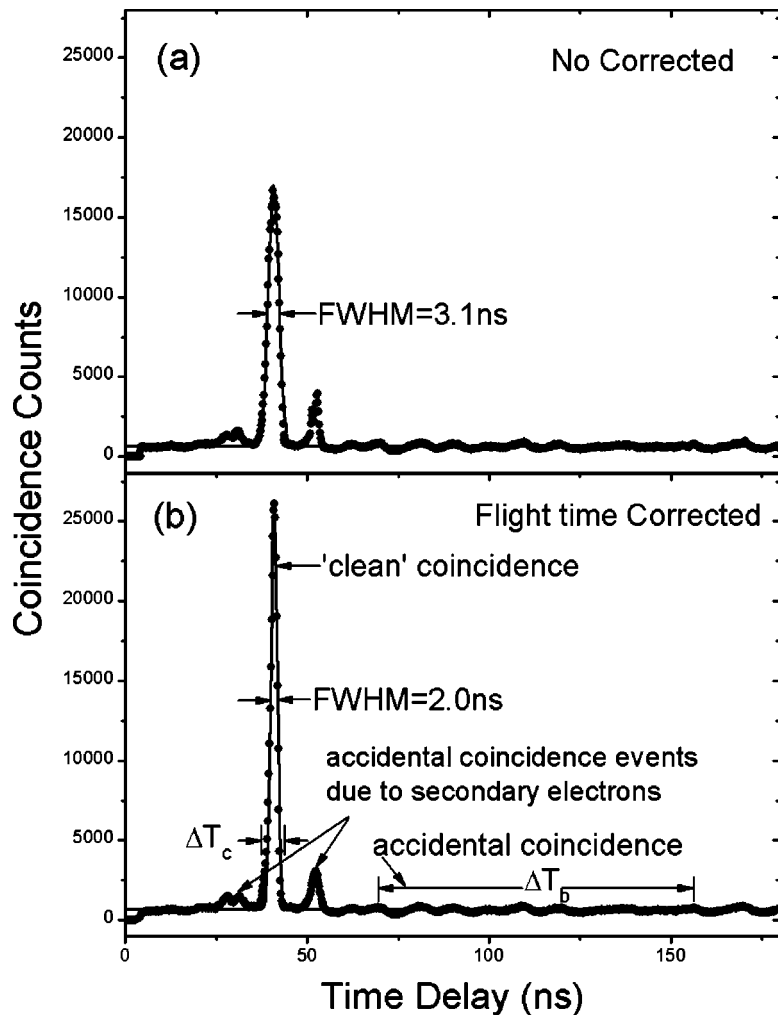
FIG. 3. Coincidence time spectra for electron flight time raw uncorrected (a) and corrected (b) data. The time resolution of 3.1 ns was improved to 2.0 ns with the correction for the flight time of the electrons in the analyzer.

of evaluating (e, 2e) cross section in terms of the electron momentum density distribution. The Dyson orbital, HF and KS momentum space wave functions can be converted into their more familiar position space counterparts and thus also into the corresponding position space orbital electron densities by Fourier transformation.

III. DESIGN OF THE APPARATUS

A cross section containing the symmetry axis of the instrument is given in Fig. 2, which consists of an electron gun, a collision chamber, a four-element conical decelerating lens with two conical apertures at the 1st and 4th electrode, the double toroidal analyzer and a pair of PSDs. A home-made electron gun equipped with a heated thoriated tungsten filament provides electron source. The incoming electron beam is well collimated by two apertures, one 1.0 mm in diameter, just outside the electron gun, the other 0.5 mm in diameter near the target gas sample. The electron beam is directed into a Faraday cup after passing through the collision chamber. Typically a current of about 20 μA is collected on the Faraday cup, which consists of an inner cup of 1 mm diameter and an outer cup. The gas jet is a nozzle of 0.5 mm diameter, which is directed toward the scattering point forming the intense target densities. Electrons leaving the (e, 2e) collision region along the conical surface at polar angle 45° are collimated with the two apertures. Both of the apertures are used to select only electrons at typically $\theta = 45° \pm 0.7°$. The two angle-selected electron beams can be decelerated by the conical lenses in order to achieve higher energy resolution. Then, the analyzer accepts those incoming beams after passing through the second apertures. About the energy analyzer Hellings et al. have used a kind of analyzer with double toroidal geometry for energy analysis.[16,17] However, the design of their energy analyzer could not be employed in the EMS spectrometer due to its very poor focusing performance in the azimuthal angle ϕ direction, while the good ϕ angle resolution is crucial for EMS measurements. The ϕ angle resolution of the developed DTA analyzer in the present EMS spectrometer has been improved greatly. The performance of resolution in energy, θ and ϕ angle have been considered simultaneously in the design of the DTA analyzer. The fringing field compensation is attempted by using Herzog plates at both the entrance and exit of the analyzer.

The energy-analyzed electrons are detected by two WSA PSDs placed behind the DTA exit aperture. One covers the azimuthal angle range from −20° to +20° and the other from 160° to 200° (as shown in Fig. 1), so the measured ϕ angle range is from −40° to +40°. The gun and analyzer systems are fabricated from 304-type stainless steel and aluminum, respectively. Apertures in the spectrometer are made of brass.
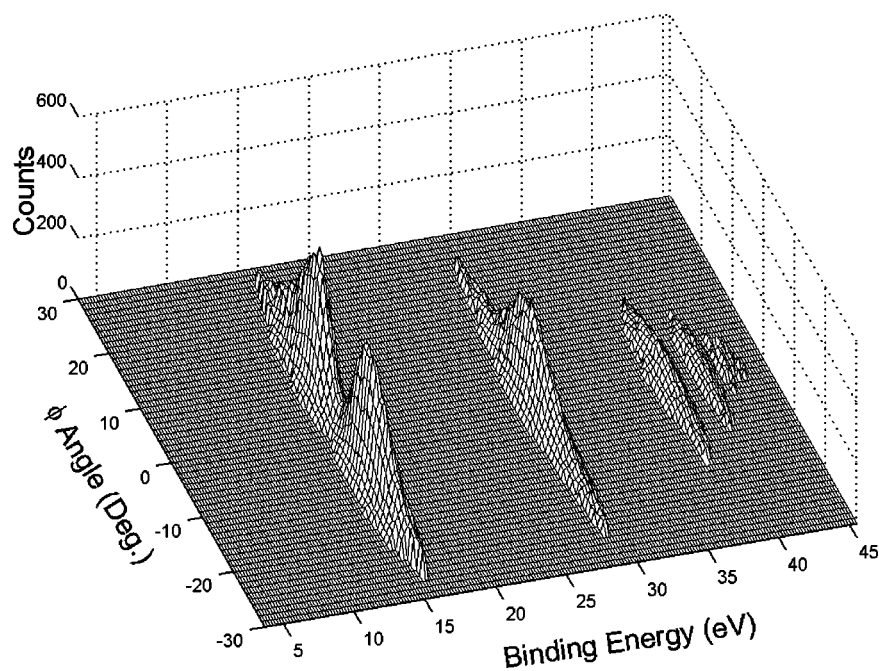
FIG. 4. Orbital electron density image of argon at $3p,3s$ and its satellite states obtained under the incident electron energy 1000 eV with the 100 eV pass energy in the analyzer.

The spectrometer is placed in a cylindrical chamber of 800 mm in diameter and 450 mm in height, and pumped by a turbo-molecular pump with a speed of 1500 L/s. The base pressure of the vacuum chamber is better than 2×10^{-7} Torr. A high-μ metal shielding is used to enclose the entire vacuum chamber in order to reduce the earth magnetic field to below 5 mG.

A digitized multi-parameter coincidence measurement system based on USB interface was used for data acquisition in the (e, 2e) spectrometer. The details of the data acquisition system have been reported previously.[14] Briefly, two WSA PSDs were used to detect the electrons. The fast timing signals are picked up via a decoupling capacitor and resistor attached to the back surface of the bottom microchannel plates (MCPs) in the chevron pair. Two fast preamplifiers are used near the vacuum chamber to inverse the timing signal from MCPs. The pulses from preamplifiers are amplified by fast amplifiers, then pass through the constant fraction discrimination (CFD) to minimize the timing jitter. The fast nuclear instrument module (NIM) logic pulse from one CFD is used as the start signal for time-to-amplitude conversion (TAC), and the signal from other CFD, after a suitable delay, as the stop signal. The amplitude of the output from TAC is proportional to the time difference between the start and the stop pulse. The charge hit on WSA is collected, respectively, from the three electrodes by charge sensitive preamplifiers, then amplified and shaped by spectroscopy amplifiers. These pulses are rather slow, but give a good signal to noise ratio.
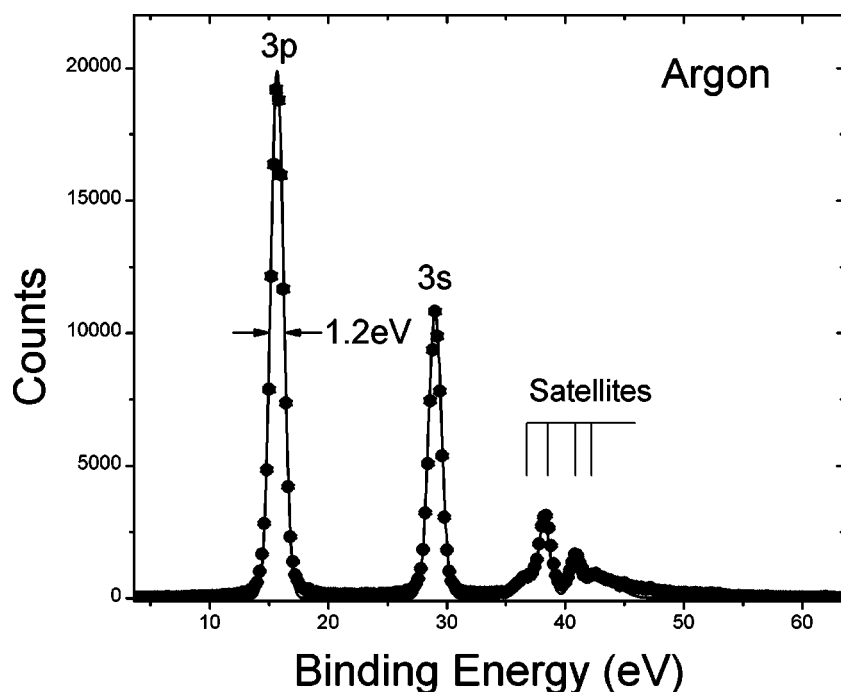
FIG. 5. The binding energy spectrum of argon obtained at an impact energy of 1000 eV plus binding energy with the 100 eV passing energy in the analyzer. The coincidence energy resolution is 1.2 eV in FWHM.
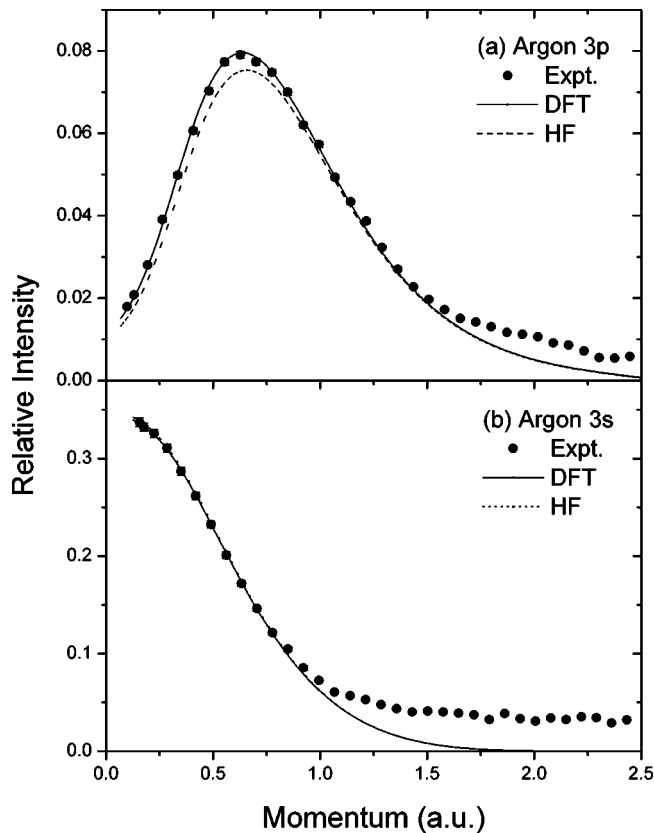
FIG. 6. Experimental and theoretical electron momentum profiles of argon for $3p$ (a) and $3s$ (b) orbitals obtained at 1000 eV incident energy. The dashed and solid lines are the associated profiles by HF and DFT theory, respectively. All the theoretical profiles are convoluted with $\Delta\theta = \pm 0.7°$, $\Delta\phi = \pm 1.9°$, and $\Delta E = 1.2$ eV.

The signals are processed by the multi-parameters system, and transferred to a computer by USB interface. To realize the USB 1.0 protocol, a microcontroller unit (MCU) and a USB interface chip were used. MCU was also used to control the system bus, and to realize the energy scan and other controls. Since MCU is programmable and directly orients the hardware, it is very flexible to realize these versatile controls with MCU. The on-line raw data are recorded on the computer hard disk, and the detailed information related to coincidence time spectra, binding energy spectra and electron momentum spectra can be obtained from the acquired raw data.

IV. CALIBRATION AND DATA REDUCTION

Calibration of the spectrometer is carried out using a mask which has a lot of narrow slits at azimuthal angles from −18° to 18° and from 162° to 198° with 6° step. The mask is mounted on the front of the decelerating lens stacks, and can be moved freely up and down. If the calibration for azimuthal angle is needed, the mask will be lifted up for obtaining the azimuthal angle ϕ of scattered electrons. In the (e, 2e) coincidence experimental mode, the mask will be moved away from the electron paths. The azimuthal angle of electrons will be kept intact during the flight because there is no field component at azimuthal direction. After collecting these electrons with known energies and angles, the calibration for PSD is achieved. The centroid for the electron position of each peak is located by a peak recognition program. The positions of electrons on PSDs with same azimuthal angle are in same radial line, and the positions of electrons on PSDs with the same energy are in the same circle. So from these lines and circles, the electron hit on the two-dimensional PSD with the x and y coordinates will be measured of its energy and azimuthal angle simultaneously.

The data produced in present EMS experiments are multidimensional. For each recorded (e, 2e) event, the raw data include the x and y coordinates of the two electrons, the arrival time difference of the two electrons and the energy of the incident electron beam. After the calibration of each detector, the electron energies and angles are readily obtained
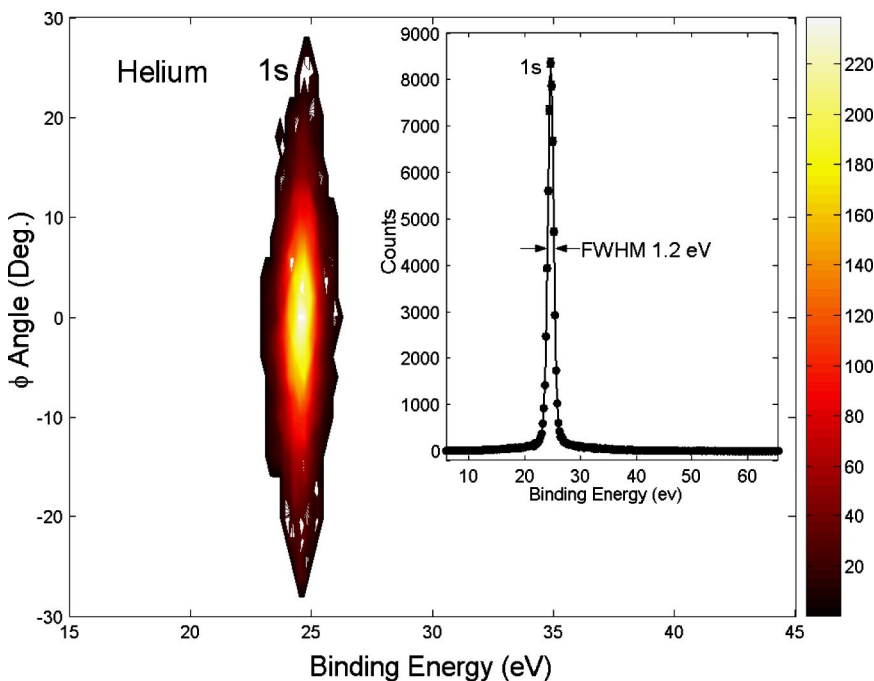
FIG. 7. (Color online) Direct EMS contour image of helium. Ground state electron density distribution at $1s$ state of helium obtained under the incident electron energy 1000 eV with the 100 eV pass energy in the analyzer. The corner shows the binding energy spectrum obtained by summing up the intensities along the x axis in the contour image. The energy resolution is 1.2 eV in FWHM.
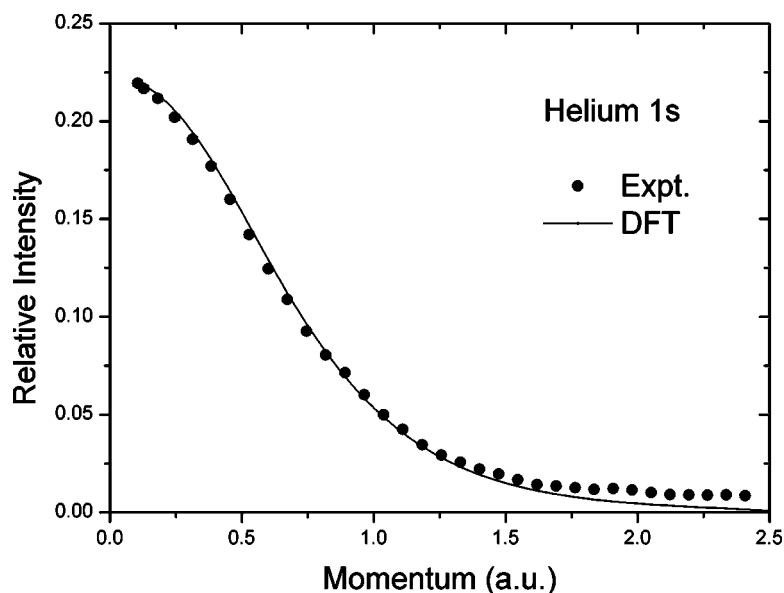
FIG. 8. Experimental and theoretical electron momentum profiles of helium 1s state obtained at 1000 eV incident energy. The theoretical profiles are convoluted with the instrumental resolutions.

using its (x,y) coordinates. The time of flight (TOF) of electrons is different when they have different energy, and the relation between TOF and electron energy can be determined by a semiempirical equation given by the electron optics simulation. So the electron energy can be used to correct the timing spectrum from the TAC. The binding energy and momentum for each event are then calculated using the electron energy of each detector and the corresponding energy of the incident beam determined by the separate voltage power supply under computer control. The full range of target electron momenta and the range of binding energies are collected in parallel.

One of the fundamental experimental results for the (e, 2e) coincidence experiment is the timing spectrum which has a significant influence on the ratio of signal to noise. The typical timing spectra for the measurement on the argon sample is shown in Fig. 3. The raw flight time and the corrected flight time spectra are shown in Figs. 3(a) and 3(b), respectively. In the current experiments the data correction was performed by software, which applies an analyzer transit

time of different electron energy to each incoming timing of (e, 2e) reaction event.[12] There are two widows set over the corrected time spectrum, one over the time interval corresponding to the true coincidences (counts N_c, width ΔT_c) with 2.0 ns full width at half maximum (FWHM), the other broad window to the accidental coincidences background (counts N_b, width ΔT_b). The accidental coincidence contribution must be subtracted from the data correlated with the coincidence peak region of the time spectrum in Fig. 3. For all recorded (e, 2e) events, the binding energy ε and the momentum $\mathbf{q}$ are determined according to Eqs. (2) and (3). The true and accidental coincidence data are stored in the respective energy and momentum array bins corresponding to small equal energy and angle intervals. The true coincidence counts, N_t, are determined by the timing information in Fig. 3. For each energy and momentum bin the data correlated with the background region of the timing spectrum, N_b, are subtracted from the data correlated with the coinci-
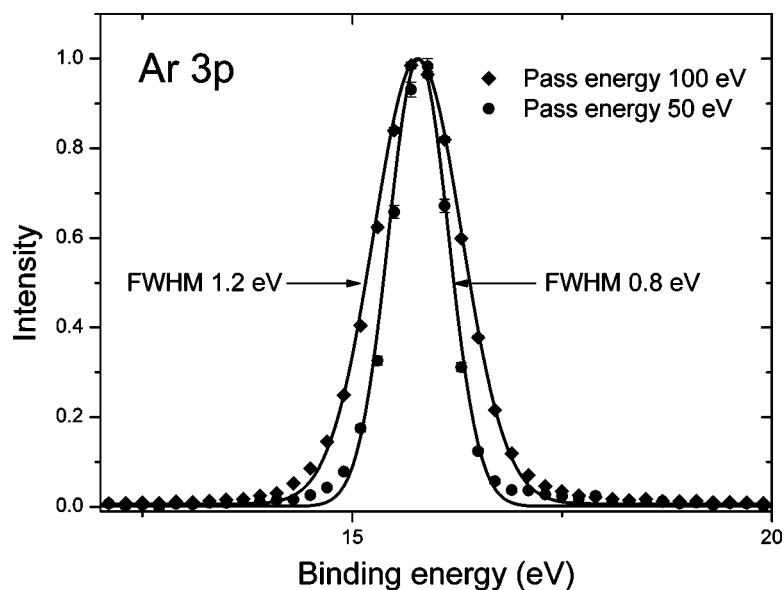
FIG. 9. Binding energy spectra of argon 3p state at 100 and 50 eV pass energy. The 1.2 and 0.8 eV energy resolutions in FWHM are obtained, respectively.

TABLE I. Comparison of performances of electron momentum spectrometers.

				Resolutions		
Year	Analyzer	Dispersivity	Monochromator	Energy (eV)	Angle (°)	Count rate
1994[a]	Cylindrical mirror analyzer	Momentum	Not used	4.3	$\Delta\phi=\pm0.5$	Moderate
1999[d]	Hemispherical analyzer	Energy	Used	0.55–0.61	1.2	Low
2000[b]	Spherical analyzer (90° sector)	Energy & momentum	Not used	2.2	$\Delta\theta=\pm0.7$ $\Delta\phi=\pm2.0$	Moderate
2002[c]	Spherical analyzer (90° sector)	Energy & momentum	Not used	2.5	$\Delta\theta=\pm0.75$ $\Delta\phi=\pm2.2$	High
This work	Double toroidal analyzer	Energy & momentum	Not used	1.2	$\Delta\theta=\pm0.7$ $\Delta\phi=\pm1.9$	High

[a]Reference 6.
[b]Reference 10.
[c]Reference 11.
[d]Reference 20.

dence region, N_c, after dividing the background counts by the background to coincidence window ratio $R(\Delta T_b = R\Delta T_c)$. That is

$$N_t = N_c - N_b/R. \qquad (7)$$

The statistical error associated with N_t is

$$\Delta N_t = \left[N_c + N_a\left(1 + \frac{1}{R}\right) \right]^{1/2}, \qquad (8)$$

where $N_a = N_b/R$ is the number of accidental coincidence counts in the coincidence timing window.

V. RESULTS AND DISCUSSIONS

Experimental argon orbital electron density distributions are shown in Fig. 4 as a function of the binding energy and azimuthal angle (i.e., electron momentum), which was measured at impact electron energy of 1000 eV plus binding energy with a 100 eV passing energy in the DTA analyzer. The entire measurement period for this complete valence shell ($3p+3s+$satellites) was only 3000 s. While the earlier typical energy dispersive EMS measurement needs 2–3 weeks (day and night). In Fig. 4, the abscissa corresponds to the binding energy and the ordinate for the azimuthal angle difference. This energy-momentum density image contains a wealth of information regarding intensities, momenta, symmetries of the various states and satellite structures. For example, traversing the image along binding energy direction yields binding energy spectra at the given angle (also, the electron momentum), and traversing parallel to the azimuthal angle axes produces the momentum distribution of the orbital at the given binding energy. The total binding energy spectrum of argon can be obtained when there is integration over all ϕ angles as shown in Fig. 5 which includes the $3p$ and $3s$ states, as well as the $3s$ satellite states resulting from electron correlation effects. It can be seen that the instrument energy resolution is about 1.2 eV FWHM at this condition; the negligibly small background contribution confirms the accuracy of the spectrometer and the procedures used in the data analysis.

Electron momentum profiles of argon $3p$ and $3s$ orbitals are shown in Figs. 6(a) and 6(b), respectively, together with associated theoretical profiles. Theoretical momentum profiles of argon have been calculated by HF and DFT. Briefly, the position-space wave functions were generated with the GAUSSIAN 98 suite program[18] by using the standard augmented correlation consistent polarized valence triple zeta (aug-cc-pVTZ) basis set and were then converted to momentum profiles with the HEMS program[7] developed at the University of British Columbia. To compare with experiments, all the profiles were convoluted with the instrumental momentum resolution ($\Delta\theta=\pm0.7°$, $\Delta\phi=\pm1.9°$, $\Delta E=1.2$ eV) according to the method in Ref. 19. The angular spread of $\Delta\theta=\pm0.7°$ is estimated by the electron trajectory simulations in the design of the spectrometer. The minimal spread of $\Delta\phi$ is $\pm1.9°$ according to experimental angle calibration and electron optic simulations when all electrodes are at optimal potentials, which is almost the same as the electron optic simulation results. The noticeable difference in angular spread between θ and ϕ comes from the fact that a toroidal analyzer has a focusing power in the θ direction, but not in ϕ. The experimental orbital electron momentum profiles of $3p$ and $3s$ orbitals were obtained by summing coincidence counts over the $3p$ and $3s$ binding energy range, respectively, and adding the data at corresponding ϕ angles for the two sets of detectors, and converting ϕ to momentum distribution by using Eq. (4). The experimental profiles in Fig. 6 exhibit rather high statistical precision, as indicated by the error bars. When compared with theoretical calculations, it can be seen that DFT calculations reproduce the experimental data better than HF. The agreement between experiment and theory is quite well at the momentum region below 1.7 a.u. for argon $3p$ and below 1.0 a.u. for argon $3s$. The discrepancies in the higher momentum region are due to the distorted wave effects, where the PWIA regime is not valid.[1] It is apparent that the spectrometer is competent to carry out extensive investigations into distorted wave effects also, for which most of the earlier EMS experiments suffered from significant uncertainties.

The contour image of the helium $1s$ orbital electron density distribution as a function of binding energy and azimuthal angle was also measured at 100 eV pass energy in analyzer with 1000 eV incident electrons over an experimental period of 600 s, as shown in Fig. 7. A binding energy spectrum of helium $1s$ ionization state has been obtained by summing up counts over all ϕ angles in the contour image, as shown in the corner of Fig. 7, which is well reproduced by the Gaussian curves with FWHM of 1.2 eV. The experimental momentum profile of helium $1s$ orbital with the theoretical calculation by DFT is shown in Fig. 8. The theoretical

profiles were convoluted with the instrumental resolution. The experimental results are obtained by summing up intensities along the ϕ angle direction in the contour image (Fig. 7) within the appropriate binding energy region of $1s$ states. A very good agreement between experiment and theory is achieved for the helium $1s$ state. Compared with the orbital momentum profile at higher momentum region of argon $3s$, it can be seen that the distortion effect become weaker in He $1s$ due to the smaller target nucleus system.

The binding energy spectra of argon $3p$ state measured at 100 and 50 eV passing energy in energy analyzer are shown in Fig. 9. The energy resolution is 0.8 eV at the 50 eV passing energy, and 1.2 eV at 100 eV passing energy, which implies that decreasing of passing energy can improve the energy resolution. The high energy resolution for argon in Fig. 9 exhibits significantly greater increase than any previously EMS measurements without using of monochromator, which indicates the high performance of the DTA analyzer.

Moreover, it is interesting to compare some important parameters between different EMS spectrometers. The comparison has been established under some circumstances, which include (i) the spectrometer performances are simultaneously obtained under a typical experimental condition, which is widely used in the future target measurements with this spectrometer, (ii) the results of target argon are chosen since argon is mostly used as a calibration sample in EMS spectrometer. The comparisons of some typical EMS spectrometers are shown in Table I.

In Table I, it is easy to see that higher count rate can be achieved by detecting on energy and momentum simultaneously, which have been obtained using the spectrometers with the spherical (90° sector)[10,11] and our double toroidal analyzers. As the comparison indicates, the performance of DTA has a better energy resolution than the spherical analyzer does. Furthermore, an energy resolution better than 0.5 eV with good angle resolutions and high count rates can be achieved under the further electron optic simulations for the DTA energy analyzer systems equipped with a monochromator, which is similar to that used in Ref. 20.

From the representative results above, the rapid and accurate images of electron density distributions will be obtained with the high sensitivity and high resolution electron momentum spectrometer using the developed DTA analyzer. And high quality data at the different experimental impact energies of 400, 600, 800, 1000, 1200, 1600, 1800, 2000 and 2400 eV can be obtained by using the present spectrometer, with which it is possible to systematically explore the dependence of the effects on the impact energy. The achieved high resolution, especially high counting rates or sensitivity, and a

wide range of (e, 2e) experimental impact energies from 400 to 2400 eV are remarkable for the future EMS. The field of EMS has long awaited such high performance and many new types of study could be carried out, such as the EMS studies in the biochemical molecules, cluster, free radicals, self-ionization and excitation state, dilute target systems, and systematically investigating of distorted wave effects. Furthermore, the fresh experimental technique in this spectrometer, especially the high performance DTA analyzer, can also be utilized for the other correlated experiments, such as the double ionization, photon excitation and ionization and the other charged particle detection experiments.

[1] I. E. McCarthy and E. Weigold, Rep. Prog. Phys. **54**, 789 (1991).
[2] C. E. Brion, Int. J. Quantum Chem. **29**, 1397 (1986).
[3] E. Weigold and I. E. McCarthy, *Electron Momentum Spectroscopy* (Kluwer/Plenum, New York, 1999).
[4] M. Vos and I. E. McCarthy, Am. J. Phys. **65**, 544 (1997).
[5] D. L. Cooper and N. L. Allan, J. Am. Chem. Soc. **114**, 4773 (1992).
[6] B. R. Todd, N. Lermer, and C. E. Brion, Rev. Sci. Instrum. **65**, 349 (1994).
[7] C. E. Brion, G. Cooper, Y. Zheng, I. V. Litvinyuk, and I. E. McCarthy, Chem. Phys. **270**, 13 (2001).
[8] J. K. Deng *et al.*, J. Chem. Phys. **114**, 882 (2001).
[9] J. H. Moore, M. A. Coplan, T. L. Skillman, and E. D. Brooks, Rev. Sci. Instrum. **49**, 463 (1978).
[10] Y. Zheng, G. Cooper, S. Tizier, B. R. Todd, and C. E. Brion, J. Electron Spectrosc. Relat. Phenom. **112**, 67 (2000).
[11] M. Takahashi, T. Saito, M. Matsuo, and Y. Udagawa, Rev. Sci. Instrum. **73**, 2242 (2002).
[12] P. Storer, R. S. Caprari, S. A. C. Clark, M. Vos, and E. Weigold, Rev. Sci. Instrum. **65**, 2214 (1994).
[13] M. Vos, G. P. Cornish, and E. Weigold, Rev. Sci. Instrum. **71**, 3831 (2000).
[14] C. G. Ning, J. K. Deng, G. L. Su, H. Zhou, and X. G. Ren, Rev. Sci. Instrum. **75**, 3062 (2004).
[15] P. Duffy, D. P. Chong, M. E. Casida, and D. R. Salahub, Phys. Rev. A **50**, 4707 (1994).
[16] G. J. A. Hellings, H. Ottevanger, S. W. Boelens, C. L. C. M. Knibbeler, and H. H. Brongersma, Surf. Sci. **162**, 913 (1985).
[17] G. J. A. Hellings, H. Ottevanger, C. L. C. M. Knibbeler, J. Van Engelshoven, and H. H. Brongersma, J. Electron Spectrosc. Relat. Phenom. **49**, 359 (1989).
[18] M. J. Frisch *et al.*, *Gaussian 98 Revision A.11.4*, Gaussian, Inc., Pittsburgh, PA, 2002.
[19] J. N. Migdall, M. A. Coplan, D. S. Hench, J. H. Moore, J. A. Tossell, V. Smith, Jr., and J. W. Liu, Chem. Phys. **57**, 141 (1981).
[20] M. J. Brunger, I. E. McCarthy, and E. Weigold, Phys. Rev. A **59**, 1245 (1999).